05,08

Destruction of uniform magnetization state in magnetic films with uniaxial anisotropy during remagnetization process

© G.M. Nikoladze, A.V. Matyunin¶, P.A. Polyakov

Moscow State University,
Moscow, Russia

¶ E-mail: physphak@mail.ru

Received September 12, 2023
Revised September 12, 2023
Accepted November 26, 2023

An experimental study of the quasi-static remagnetization process in ferrite-garnet film with both in-plane and uniaxial anisotropy by a rotating magnetic field has been carried out. With the help of an original magneto-optical setup, using the Faraday effect, it was shown that the uniform magnetization state is destructed in narrow regions, where the magnetic field vector's direction is close to the hard axis' direction. The theory that agrees well with the experimental results is proposed.

Keywords: thin magnetic films, uniaxial anisotropy, quasi-static remagnetization, magneto-optics, domains.

DOI: 10.21883/0000000000

1. Introduction

Physical principles of operation of various spintronics devices are based on remagnetization of uniformly magnetized thin magnetic layers. For example, nanothick magnetic stripes connected in series are used in anisotropic magnetoresistance effect sensors of magnetic field [1–6]. Spin-valve and spin-tunnel devices use multilayer magnetic structures [7–13]. Maximum possible uniform remagnetization of magnetic layers shall be achieved to ensure stable operation of these devices. Experimental study of the quasi-steady-state remagnetization of planar-anisotropy magnetic films with uniaxial anisotropy in the film plane was conducted herein. Areas where homogeneous magnetization failure and domain structure occurrence take place were detected. Theoretical interpretation of this phenomenon is offered.

2. Experimental setup description

For the experimental studies, an original magneto-optical setup described in detail in [14] was used. General view of the setup is shown in Figure 1. The detail in Figure 1 shows the system of coils creating magnetic fields required for comprehensive experimental investigations. Remagnetization processes in the film under study are initiated using large coils *2* (axis *X*) are used to create the remagnetization field (up to 40 Oe), by means of which end position of the magnetization vector can be set; and small coils *3* capable of creating fields up to 16 Oe (axis *Z*) that are used to compensate Earth's field and to provide the magnetization vector necessary to observe the Faraday effect (because the magnetization vector goes from the film plane by max. 5°).

Using interface unit *4* (software-controlled from laptop *7*), field configurations may be created for experimental studies (with pre-defined field strengths that may be varied in 0.1 Oe increments). The switch unit is connected to power supply *5* (*Mastech HY3003*) which is necessary to energize the required field configurations (additional similar power supply *6* may be involved to create higher strength fields). Field strengths are monitored by magnetometer *9* (*LIS3MDL*). The domain structure images are recorded using digital camera *10* (*Nikon D3400*).

3. Experimental results

Using the experimental setup described above (Figure 1), the quasistatic remagnetization of ferrite-garnet film by

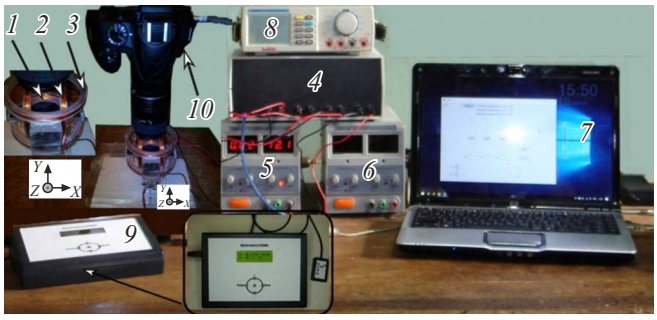

Figure 1. General view of the magneto-optical setup. *4* — switch unit, *5* — switch unit power supply (*Mastech HY3003*), *6* — additional power supply of the switch unit (*Mastech HY3003*), *7* — laptop, *8* — multimeter for coil circuit current monitoring (*Mastech M9803R*), *9* — magnetometer (*LIS3MDL*), *10* — digital camera for domain structure recording (*Nikon D3400*). Detail in Figure 1: *1* — small coils mainly used for saturation of the film under study, *2* — large coils creating the remagnetization field, *3* — small coils used for Earth's field compensation and creating the magnetization vector component required for observation of the Faraday effect.

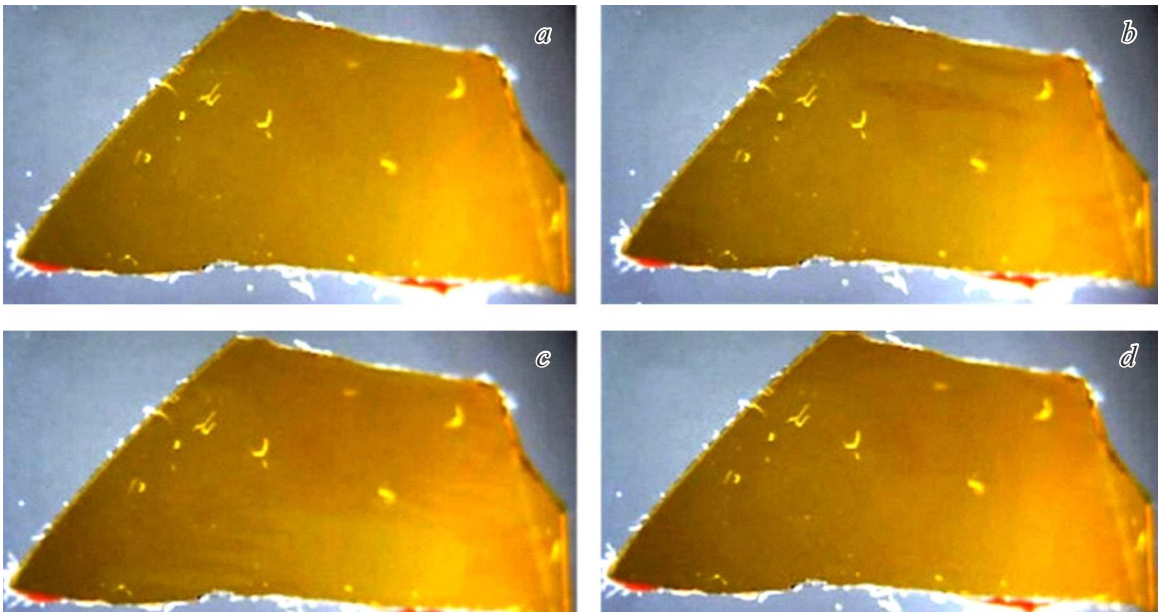

Figure 2. Magnetooptical images of the magnetic structure of ferrite-garnet film with different orientations of the magnetic field strength vector. *a* — the film is uniformly magnetized by $H_0 = 4$ Oe; *b* — domain structure initiation time when the angle of 4 Oe magnetic field vector **H** is equal to 79°; *c* — film domain structure occurring at vector angle 85°; *d* — domain structure occurring in the film when the angle of vector **H** is equal to 95°.

external rotating magnetic field is studied herein. The rotating magnetic field is created by two Helmholtz coils placed perpendicular to each other as shown in Figure 1. A sample with the following parameters (typical or similar materials [15]) was used: saturation magnetization $M_S = 14$ G; technical saturation field $H_{sat} = 2.5$ Oe; effective planar anisotropy field $H_{K_p} = 1100$ Oe; film composition — $(LuBi)_3(FeGa)_5O_{12}$; thickness $d = 4\,\mu$m. The film was trapezoid with transverse dimensions ≈ 1 cm (Figure 2). Magnetic structure in the film was observed by the Faraday magneto-optic effect. Polarized light going through the magnetized film area that is slightly inclined (about 15°) rotates its polarization plane at some angle proportional to the magnetization vector projection on the light beam direction. The size of this projection will depend on the magnetization orientation in the film plane. When the film is observed through a polaroid, different light intensity will be recorded for the light that has passed through the film areas with different magnetization orientation, i. e. domain structure of the film will be recorded. Approximately uniform illumination of the film is observed during uniform magnetization. Figure 2 shows magneto-optic images of magnetic domain structures of the film remagnetized in the rotating magnetic field.

Before the measurement, the film was uniformly magnetized in $H_0 = 4$ Oe magnetic field oriented horizontally from left to right (Figure 2, *a*). The film was illuminated uniformly. Then the magnetic field was quasistatically rotated counterclockwise in the film plane at 360°. As a result, destruction of the uniform magnetization and domain ordering were detected in some angle range. Figure 2, *b* shows the domain structure initiation time at an angle of 4 Oe magnetic field vector **H** equal to 79°. Dark extended sharpened regions (domains) with different magnetization vector orientation **M** can be seen clearly. Vector orientations **M** within and outside the domain shall be opposite and directed approximately along the easy magnetization axis (EMA). Therefore orientation of the sharpened domain in Figure 2, *b* shows the direction of EMA which is inclined with respect to horizontal approximately at 10°−11°. Figure 2, *c* shows the domain structure that occurs in the film under study when 4 Oe magnetic field vector **H** is rotated at 85°. It can be seen that the film is more than by half remagnetized to the opposite orientation with respect o EMA. When vector **H** of this magnetic field is rotated at 95°, the film is completely remagnetized and becomes uniformly magnetized which is confirmed by an approximately uniform light background of the whole film surface (Figure 2, *d*). With further quasistatic rotation of magnetic field vector **H** (in rotation angle range 260°−274°), the uniform magnetization state is destroyed and then domain ordering occurs which is similar to that shown in Figure 2, *b* and *c*. It should be noted that the domain ordering regions are located almost symmetrically, i. e. approximately coincide at 180°.

The Table shows rotation angles φ_1 of vector **H** according to field strength $H_p = |\mathbf{H}|$ at which the first destruction of the uniform magnetization state and initiation of wedge-shaped magnetic domains occur (see Figure 2, *b*). At φ_2, the uniform magnetization state of the film is restored, i. e.

Experimental boundary angles of the magnetic field strength vector at which the uniform magnetization state is destroyed and restored

H_p,Oe	φ_1,°	φ_2,°	φ_3,°	φ_4,°	$\varphi_2-\varphi_1$,°	$\varphi_4-\varphi_3$,°
4.0	79.0	95.0	260.0	274.0	16.0	14.0
9.6	80.0	88.0	260.0	268.0	8.0	8.0
14.7	80.0	86.0	260.0	266.0	6.0	6.0
20.1	80.0	85.0	260.0	265.0	5.0	5.0
25.4	80.0	84.0	260.0	264.0	4.0	4.0
31.3	80.0	83.0	260.0	263.0	3.0	3.0
36.4	80.0	83.0	260.0	263.0	3.0	3.0
39.9	80.0	83.0	260.0	263.0	3.0	3.0

the film is uniformly magnetized through the movement of domain boundaries. The second destruction of the uniform magnetization state occurs at φ_3, and at φ_4 the uniform magnetization state of the film is restored again.

The experimental data listed in the Table shows that the regions of the uniform magnetization state destruction and of the magnetic domain ordering occur in two angle ranges: $\varphi_2-\varphi_1$ and $\varphi_4-\varphi_3$. These regions decrease with an increase in magnetic field strength H. With an increase in the magnetic field from 4 to 39.9 Oe, the angle range at which the domain structure is observed decreases in the first range from 16 to 3° and in the second range — from 14 to 3°. It should be noted that, except the magnetic field strength of $H_p = 4$ Oe, at all other strengths H_p the uniform magnetization state ranges of the first and second regions coincide. Boundary angles φ_1, φ_2 and φ_3, φ_4 differ by 180°, except for the first values at $H_p = 4$ Oe.

4. Theoretical interpretation of the experimental findings

Figure 3 shows the horizontal axis X of the Cartesian axes system about which angle φ of magnetic field vector **H** is counted. Orientation of the easy magnetization axis (EMA) is deviated at $\alpha = 10°$ with respect to the axis X in accordance with the wedge-shaped domain orientation in Figure 2, *b*. Then, considering the numerical values of φ_1 and φ_2, as listed in the Table, we come to a conclusion that the uniform magnetization state is destroyed when the external magnetic field strength is oriented along the hard magnetization axis (HMA).

For interpretation of the experimental data, we will assume that the uniform magnetization state of the film is destroyed with rotation of external magnetic field vector **H** when the hard magnetization axis orientation is achieved. With further rotation of vector **H**, domains with the opposite orientation of magnetization vector **M** about the easy axis are growing, which is shown in magneto-optic images in

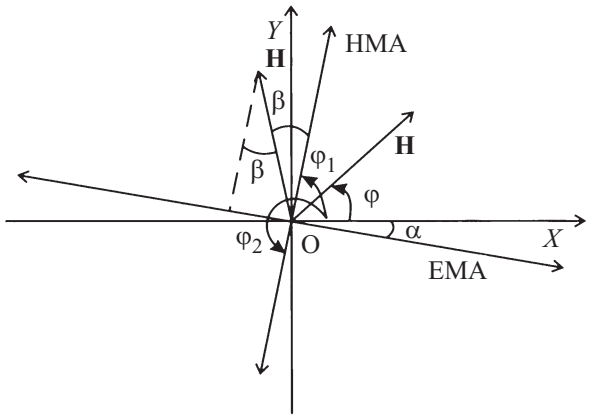

Figure 3. Orientation of easy magnetization axes (EMA) and hard magnetization axes (HMA) with respect to the horizontal axis X from which rotation of magnetic field vector **H** is counted.

Figure 2, *b, c*. When rotation angle $\varphi_2 = \beta + \varphi_1$ is achieved (see Figure 3), full film remagnetization occurs through the domain boundary (DB) movement. DB movement itself is caused by the magnetic field component along EMA equal to, as shown in Figure 3,

$$|\mathbf{H}| \cdot |\sin\beta|. \tag{1}$$

In the angle range from φ_1 to φ_2, equilibrium domain structures, where ponderomotive force caused by field (1) is compensated by the DB tension force and magnetostatic field, are observed. However, when the field component achieves some critical state H_{cr}, this compensation becomes impossible and full remagnetization of the film occurs due to the domain boundary movement mechanism. According to the foregoing, relation for full film remagnetization and restoration of the uniform magnetization state may be written as

$$|\mathbf{H}| \cdot |\sin\beta| = H_{cr}. \tag{2}$$

Here, β is the angle (in radians) between vector **H** and hard magnetization axis orientation (Figure 3).

According to the experimental data, $\beta \ll 1$, therefore relation (2) may be approximately written as

$$H \cdot \beta = H \cdot \beta^\circ \cdot \pi/180^\circ = H_{cr}, \tag{3}$$

where β° is the angle in degrees (the values are found by means of the table review). We get

$$H \cdot \beta^\circ = H_{cr} \cdot 180^\circ/\pi = \overline{H}_{cr} = \text{const}. \tag{4}$$

It should be noted that new constant $\overline{H}_{cr}$ in the above-mentioned equation has the dimension „oersted multiplied by degree“ (Oe $\cdot^\circ$). From relation (4), we get a simple theoretical dependence of the angle range (in degrees), where the uniform magnetization state of the film is destroyed, on the external magnetic field strength

$$\beta^\circ = \overline{H}_{cr}/H. \tag{5}$$

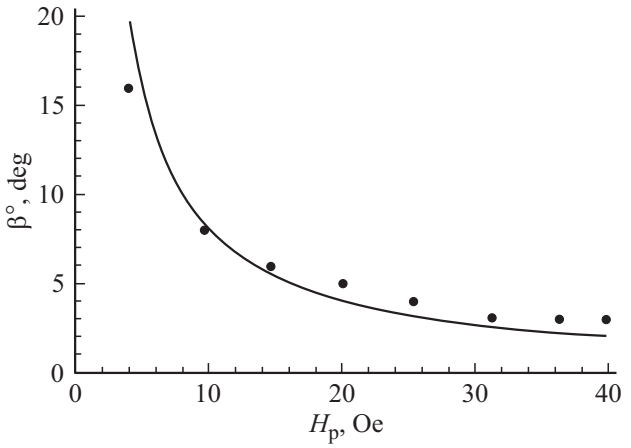

Figure 4. Theoretical dependence of the nonuniform magnetization region width β° in the film on the remagnetizing field H_p with applied experimental data.

Value of $\overline{H}_{cr}$ may be obtained from the experimental data listed in the Table. By multiplying the values of the first and penultimate columns and by averaging the calculated values we find that $\overline{H}_{cr} = 80.6\,\text{Oe}\cdot^\circ$. By similar calculations for the second range of the uniform magnetization state destruction (using the data from the last column of the table), we find that in this case $\overline{H}_{cr} = 79.6\,\text{Oe}\cdot^\circ$. By averaging these two values, we will finally obtain the following value:

$$\overline{H}_{cr} = 80\,\text{Oe}\cdot^\circ. \quad (6)$$

Curve of theoretical dependence (5) of the angular region of the uniform magnetization state destruction β° on the remagnetization field H_p under condition (6) and the corresponding dependence derived from the table are shown in Figure 4.

Figure 4 shows that the theoretical dependence of the region where the uniform magnetization state is destroyed coincides quite well with the obtained experimental data.

5. Conclusion

As specified in the Introduction, uniformly magnetized film magnetic elements are used in many spintronics devices. However, it is important for normal operation of these devices that these film elements should be uniformly remagnetized under the magnetic field exposure. Investigations conducted herein have shown that there are conditions under the magnetic field exposure when the uniform magnetization state is destroyed. The findings and established patterns may assist developers in avoiding these undesirable film element remagnetization conditions.

Conflict of interest

The authors declare that they have no conflict of interest.

References

[1] E. Demirci. J. Supercond. Nov. Magn. **33**, 3835 (2020).
[2] Chenying Wang, Wei Su, Zhongqiang Hu, Jiangtao Pu, Mengmeng Guan, Bin Peng, Lei Li, Wei Ren, ZiyaoZhou, Zhuangde Jiang, Ming Liu. IEEE Trans. Magn. **54**, *11*, 1 (Art no. 2301103) (2018).
[3] P.V. Sreevidya, Jakeer Khan, Harish C. Barshilia, C.M. Ananda, P. Chowdhury. JMMM **448**, 298 (2018).
[4] Chong-Jun Zhao, Min Li, Jian-Wei Li, Lei Ding, Jiao Teng, Guang-Hua Yu. JMMM **368**, 328 (2014).
[5] Lisa Jogschies, Daniel Klaas, Rahel Kruppe, Johannes Rittinger, Piriya Taptimthong, Anja Wienecke, Lutz Rissing, Marc Christopher Wurz. Sensors *15*, 28665 (2015).
[6] V.V. Amelichev, D.A. Zhukov, S.I. Kasatkin, D.V. Kostyuk, O.P. Polyakov, P.A. Polyakov, V.S. Shevtsov. Pisma v ZhTF **47**, *10*, 19 (2021). (in Russian).
[7] Van Su Luong, Anh Tuan Nguyen, Quoc Khanh Hoang, Tuyet Nga Nguyen, Anh Tue Nguyen, Tuan Anh Nguyen, Van Cuong Giap. J. Sci.Adv. Mater. Dev. **3**, *4*, 399 (2018).
[8] V.P.C. Limeira, L.C.C.M. Nagamine, J. Geshev, D.R. Cornejo, F.J. Garanhani. J. Phys.: Condens. Matter **31**, *26*, 1 (Art no. 265802) (2019).
[9] Sadhana Singh, Pawan Kumar, Ajay Gupta, Dileep Kumar. JMMM **513**, 1 (Art no. 167186) (2020).
[10] Si Nyeon Kim, Jun Woo Choi, Sang Ho Lim. Sci. Rep. **9**, 1 (Art no. 1617) (2019).
[11] Sabpreet Bhatti, Rachid Sbiaa, Atsufumi Hirohata, Hideo Ohno, Shunsuke Fukami, S.N. Piramanayagam. Mater. Today **20**, *9*, 530 (2017).
[12] V.V. Amelichev, D.V. Vasiliev, P.A. Polyakov, D.V. Kostyuk, P.A. Belyakov, S.I. Kasatkin, O.P. Polyakov, Yu.V. Kazakov. FMM **124**, *5*, 1 (2023). (in Russian)
[13] L.I. Naumova, M.A. Milyaev, R.S. Zavornitsyn, A.Yu. Pavlova, I.K. Maksimova, T.P. Krinitsina, T.A. Chernyshova, V.V. Proglyado, V.V. Ustinov. FMM **120**, *7*, 710 (2019). (in Russian).
[14] A.V. Matyunin, G.M. Nikoladze, P.A. Polyakov. Izv. RAN, Ser. fiz. **86**, *9*, 1239 (2022). (in Russian).
[15] O.S. Kolotov, A.V. Matyunin, G.M. Nikoladze, P.A. Polyakov. FTT *10*, 1892 (2017). (in Russian).

Translated by E.Ilinskaya